ELSEVIER

International Journal of Mass Spectrometry 220 (2002) 145–158

International Journal of Mass Spectrometry

www.elsevier.com/locate/ijms

Complete chemical conversion of $[(NO)_m(CH_3OH)_n]^+$ to $NO^+(CH_3ONO)_{x(x=1-12)}$: experiment and theory

Dong Nam Shin [a], Thomas R. Furlani [b], Robert L. DeLeon [b], James F. Garvey [b,*]

[a] *Department of Chemistry, Colorado State University, Ft. Collins, CO 80523-1872, USA*
[b] *Department of Chemistry, University at Buffalo, The State University of New York, Buffalo, NY 14260-3000, USA*

Received 2 October 2001; accepted 3 January 2002

Abstract

We have observed the complete conversion of clusters containing NO and CH_3OH to methyl nitrite (CH_3ONO) ionic clusters, via 248 nm multiphoton ionization. The mass spectrum exhibits a characteristic pattern such that there are cluster ions containing solely CH_3ONO of the type $(NO)^+(CH_3ONO)_x$ ($x = 1$–12). Expected cluster ions such as $(CH_3OH)_mH^+$ (for $m > 3$) or $(NO)_n{}^+$ (for $n > 3$) are not observed. The present work reports the first experimental observation showing the complete chemical conversion of reagent molecules within the environment of a cluster ion. A discussion, supported by calculations, of possible reaction mechanisms responsible for the facile generation of the methyl nitrite cluster species is also presented. (Int J Mass Spectrom 220 (2002) 145–158)

Keywords: Multiphoton; Ionization; Mass spectrum; Cluster ions; Methyl nitrite; Nitric oxide; Methanol

1. Introduction

During the past decade there have been a number of investigations of the elimination of nitrogen oxides from various industrial processes due to their central role in environmental problems [1] such as acid rain and photochemical ozone formation in the troposphere as well as the ozone layer depletion in the stratosphere. As a result, there is an ongoing effort to abate the emission of nitrogen oxides (NO_x) in the atmosphere [2–11]. This effort has involved experiments both to examine the chemical mechanisms involved in $DeNO_x$ processes [12–15] and to understand the operational parameters of current $DeNO_x$ systems [16,17].

Recently, electron-beam [8–11] and corona discharge [10,11] generated non-thermal plasmas offer promising new techniques for the abatement of NO_x in atmospheric pressure flue gas streams. In these methods, the key step is the initial conversion of NO to NO_2, since NO_2 is much more reactive as well as soluble in water and can be readily removed. Any new method, however, must be based on both technical and economical factors as prerequisites for its possible practical application [18]. As a result, additives such as hydrocarbons [19–21], ammonia [22,23], hydrogen peroxide [24,25] and alcohols [21,26] have all been studied in order to attempt to improve the overall efficiency of $DeNO_x$ processes.

Methanol, of all the additives, appears to be a highly attractive possibility. Methanol [6,21,27,28] is capable of generating powerful oxidants such as HO_2,

---

[*] Corresponding author. E-mail: garvey@chem.buffalo.edu

1387-3806/02/$ – see front matter © 2002 Elsevier Science B.V. All rights reserved.
PII S1387-3806(02)00770-4

CH_3O_2 and HCO_3. The oxidation of NO to NO_2 in the presence of methanol has been explored previously in thermal $DeNO_x$ processes [6,27,28], where the temperature of the system is as high as 1000 K. In contrast with thermal $DeNO_x$ processes, the use of methanol in non-thermal plasma processes is currently under investigation [21].

One of main concerns in the post-treatment of flue gas cleaning, via non-thermal plasmas, is the influence of the ions generated by the plasma. Recently, Matzing [9] used over 800 elementary reactions to describe the detailed chemical reaction mechanism responsible for flue gas cleaning by non-thermal plasma. Over 500 of these elementary reactions are related to ion chemistry. In addition to these gas phase ionic reactions, it has recently been reported that cluster and heterogeneous reactions can also exert significant influence upon flue gas cleaning [29–31]. For instance, the NO_x removal efficiency is significantly enhanced when water is present within the gas mixture [31]. It is considered to be primarily due to the formation of $NO^+(H_2O)_n$ and $NO_2{}^+(H_2O)_n$ [32–34], followed by conversion into nitrous and nitric acids, respectively. Observing ion chemistry within gas phase clusters can be a useful method to explore possible reactive processes that are expected to occur within the $DeNO_x$ process.

Recently, we have reported the observation [35] that one can generate mixed cluster ions of the type $[(NO)_n(CD_3O)_x(CD_3OH)_m]^+$, containing multiple methoxy radicals. The structure of these cluster ions has been suggested to be $[(NO)_{n-x}(CD_3ONO)_x(CD_3OH)_m]^+$ containing methyl nitrite. In this paper, we have observed not only (i) more conclusive evidence that methyl nitrite species are generated within the cluster ions, but also (ii) the complete conversion of neutral clusters, $(NO)_m(CH_3OH)_n$, into $[(NO)(CH_3ONO)_x]^+$ cluster ions, via 248 nm multiphoton ionization. The observation of this conversion demonstrates the possibility of generating methyl nitrite in $DeNO_x$ processes when methanol is used as an additive in non-thermal plasma techniques. Lastly, the chemical reaction mechanisms behind the selective formation of the cluster ions containing methyl nitrite molecules such as $[(NO)(CH_3ONO)_x]^+$ are discussed in terms of both a stepwise and a concerted mechanism.

2. Experimental and computational methods

A detailed description of our reflectron time-of-flight mass spectrometer (RTOFMS, Jordan Co.) has been provided elsewhere [36,37]. In brief, the neutral heteroclusters were expanded through a commercial pulsed nozzle (General Valve Co., IOTA ONE) with an 800 μm orifice diameter. After skimming the resulting expansion by a 1.0 mm conical skimmer located 1.5 cm away from the nozzle, the cluster beam was introduced into the ionization region of the RTOFMS and then irradiated by an unfocused 248 nm laser beam (Lambda Physik, EMG101) with typical laser energy below 3.4 mJ per pulse. Cluster ions generated by the laser pulse were accelerated in a double electrostatic field to 4.2 kV and traveled through a 140 cm long flight tube, reflected by a double stage reflectron located at the top of the flight tube. Following the reflectron, the ions travel for an additional 61 cm to a dual microchannel plate detector. The background pressure in the flight tube of the mass spectrometer was maintained below 5×10^{-7} Torr to reduce collision-induced dissociation by using both a 370 L/s turbo molecular pump and a liquid nitrogen cryo-pump. The pressure in the source region is raised to 5×10^{-6} Torr during normal molecular beam operation and the detected ion signals were recorded by a transient digitizer (LeCroy 9310A).

Experiments are typically performed with a gas mixture consisting of 0.1–0.7% CH_3OH (or 0.08–0.59% CD_3OH) and 5.0% nitric oxide in 3.0 atm of Ar carrier gas. CH_3OH (Fisher Chemical Co., 99.9%) and CD_3OH (Cambridge Isotope Laboratory, D 99%) were used. The 5.0% premixed nitric oxide gas seeded in Ar was obtained from Matheson Gases. All of these reagents were used without further purification.

All quantum chemical ab initio calculations were performed with the Gaussian 98 package program [38]. The geometries of all species considered in this study have been optimized at the MP2(full)/6-31G (d,p) level of theory, where ‘full’ denotes the inclusion of all electrons. Normal mode analyses were also carried out to characterize the nature of stationary points and to determine zero-point vibrational energy (ZPVE). For anharmonicity correction, the calculated ZPVE values were scaled by 0.93. Intrinsic reaction coordinate (IRC) was performed to verify transition structures connecting the desired reactant and product. Single-point energies were also calculated with the G2 procedure using MP2(full)/6-31G(d,p) optimized geometries to achieve more accurate energetic data [39].

3. Experimental results

Fig. 1 shows a typical mass spectrum of a NO/CH_3OH mixture (at a methanol concentration of 0.7%) in the mass region from 60 to 780 amu. The mass spectrum is remarkably simple, consisting of a series of intense peaks separated by 61 amu, attributed to the $[(NO)(CH_3ONO)_x]^+$ cluster ion series. In our preceding paper [35], we confirmed, through isotopic substitution, that hydrogen atom loss from the methanol occurs from the hydroxyl group. Therefore, the repeating unit of 61 amu in the NO/CH_3OH cluster system is attributed to the production of CH_3ONO (rather than $ONCH_2OH$). This nearly complete conversion of NO/CH_3OH to $(NO)^+(CH_3ONO)_x$ through the selective dissociation of the O–H bond, is found to persist over the entire range of CH_3OH concentrations employed in the present study.

As shown in Fig. 2, an expansion of Fig. 1, a variety of smaller ion peaks appears between the strong ion series, $[(NO)(CH_3ONO)_x]^+$. These additional

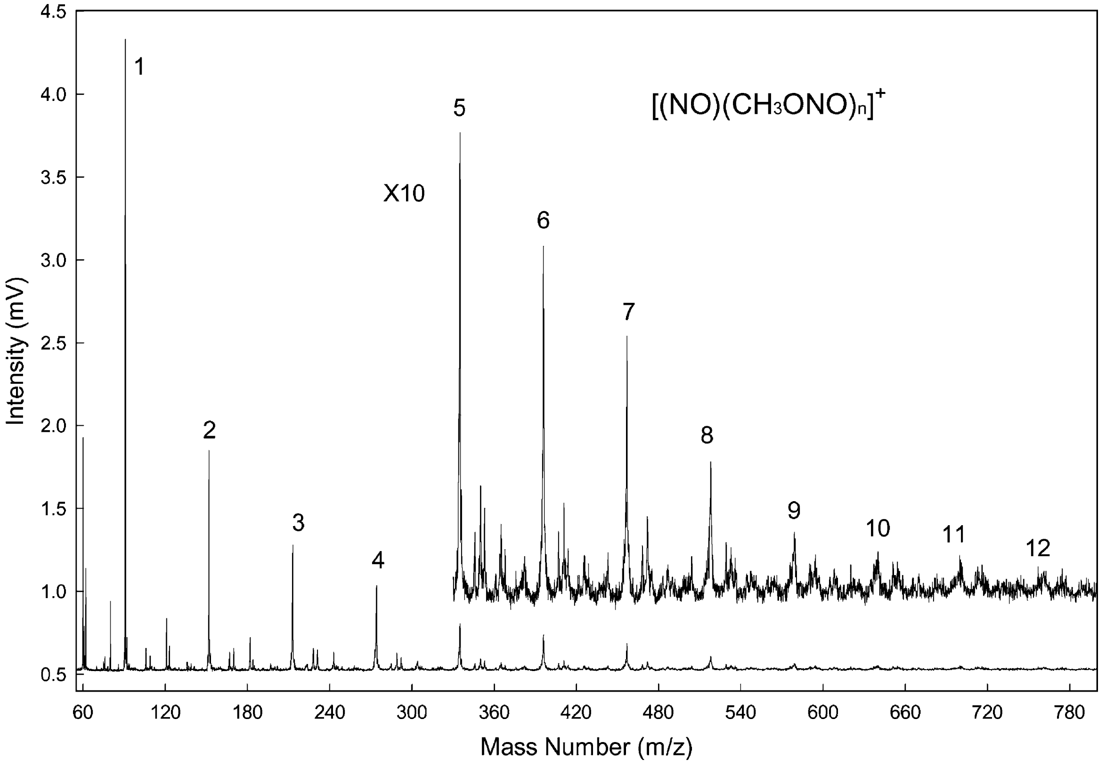

Fig. 1. Typical mass spectra of an expansion of NO (5%) and CH_3OH (0.7%) mixed cluster in 3.0 atm of Ar carrier gas. The number on each peak represents the number of methyl nitrite (CH_3ONO) molecules, in a given cluster ion of the form $[(NO)(CH_3ONO)_n]^+$. Note that the repeating unit of m/z 61, corresponding to the methyl nitrite species, is observed in the mass spectrum.

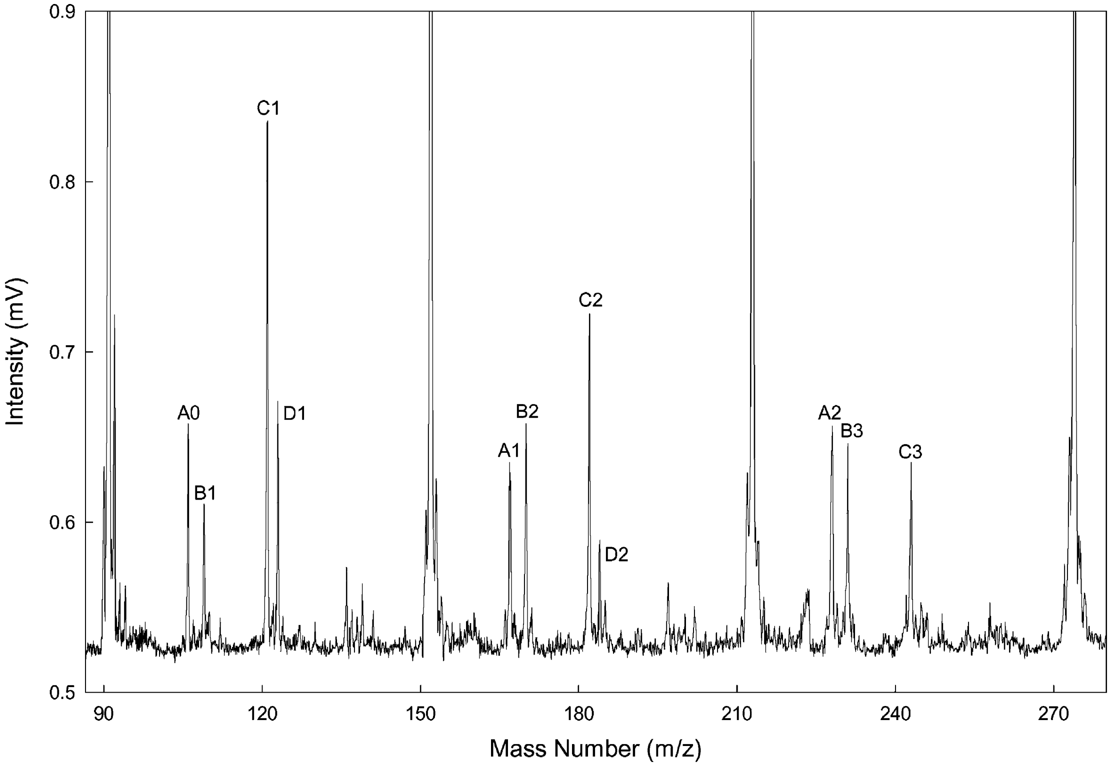

Fig. 2. The mass spectrum between 90 and 270 amu is shown in more detail. The cluster ion series between $[(NO)(CH_3ONO)_{x-1}]^+$ and $[(NO)(CH_3ONO)_x]^+$ are indicated as follows: $[(NO)_2(NO_2)(CH_3ONO)_a]^+$ (for $a = 0$–10); $[(NO)(H_2O)(CH_3ONO)_b]^+$ (for $b = 0$–11); $[(NO)_2(CH_3ONO)_c]^+$ (for $c = 0$–6); and $[(NO)(CH_3OH)(CH_3ONO)_d]^+$ (for $d = 0$–3).

cluster ion series are readily assigned as $[(NO)_2(NO_2)(CH_3ONO)_a]^+$ (for $a = 0$–10), $[(NO)(H_2O)(CH_3ONO)_b]^+$ (for $b = 0$–11), $[(NO)_2(CH_3ONO)_c]^+$ (for $c = 0$–6) and $[(NO)(CH_3OH)(CH_3ONO)_d]^+$ (for $d = 0$–3). We note that these cluster ion series also contain mainly CH_3ONO molecules.

In order to rule out fission of the C–H bond in the methanol as a possible source of H atom loss, we obtained spectra using CD_3OH. Fig. 3 shows a set of mass spectra for NO/CD_3OH mixture, as a function of methanol concentration. The spectrum reveals four peaks at m/z 62, 64, 65 and 66. These are readily identified as $[(NO)(CD_2O)]^+$, $[(NO)(CD_3O)]^+$, $[(NO)(CD_3OH)]^+$, and $[(NO)(CD_3OH)]H^+$ (or $[(NO)(CD_3OD)]^+$), respectively. It is striking there is no evidence of the $[(NO)(CD_2OH)]^+$ cluster ion. There is, however, an intense peak $[(NO)(CD_2O)]^+$ corresponding to loss of an H and a D atom. Fig. 4 shows similar mass spectra at a higher mass range. The mass spectra are displayed, against the number of NO molecules within cluster ions of the form $[(NO)_m(CD_3OH)]^+$. It also should be emphasized that the cluster ions losing only one D atom from the methyl group are absent for the larger cluster ions comprising two or more NO molecules. On the basis of these observations obtained from both NO/CH_3OH and NO/CD_3OH clusters, we believe there is a strong preference for selective O–H bond dissociation in NO/methanol cluster ions as an initial reaction channel. There may then follow further dissociation of a C–H (or C–D) bond to produce formaldehyde CH_2O from CH_3OH (or CD_2O from CD_3OH).

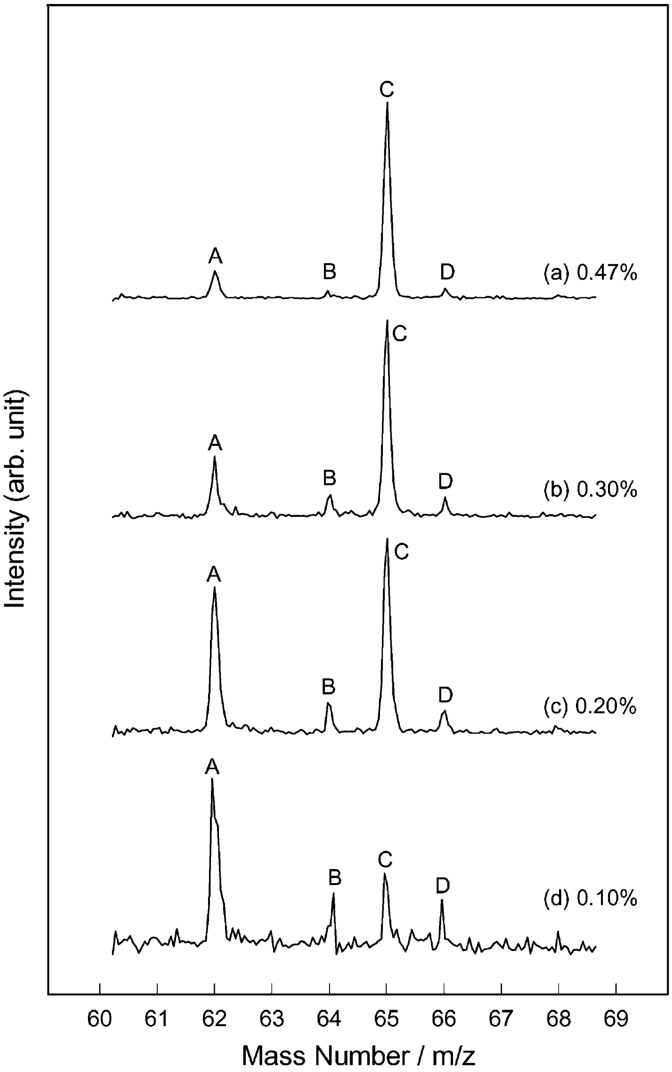

Fig. 3. Cluster ion mass spectra obtained for a mixture of NO (5%) and CD_3OH (from top 0.47, 0.30, 0.20, and 0.10%) seeded in 3.1 atm of Ar carrier gas. The peaks are identified as follows: (A) $[(NO)(CD_2O)]^+$; (B) $[(NO)(CD_3O)]^+$; (C) $[(NO)(CD_3OH)]^+$; (D) $[(NO)(CD_3OH)]H^+$ or $[(NO)(CD_3OD)]^+$.

4. Discussion

4.1. Stepwise and concerted reaction mechanisms

Ionic clusters containing methyl nitrite molecules are observed to be the major cluster ion series resulting from the ionization of neutral NO/methanol clusters. Neat clusters of the type $(CH_3OH)_nH^+$ and $(NO)_n{}^+$ are not observed in this study, except for a small amount of the $(NO)_2{}^+$ ion. In our previous study, using a high concentration of methanol [35], we were able to observe homogeneous cluster ions of both the protonated methanol and nitric oxide species as well as the heterogeneous cluster ions containing methyl nitrite as major ion peaks. This new study has demonstrated that the relative concentration within the binary

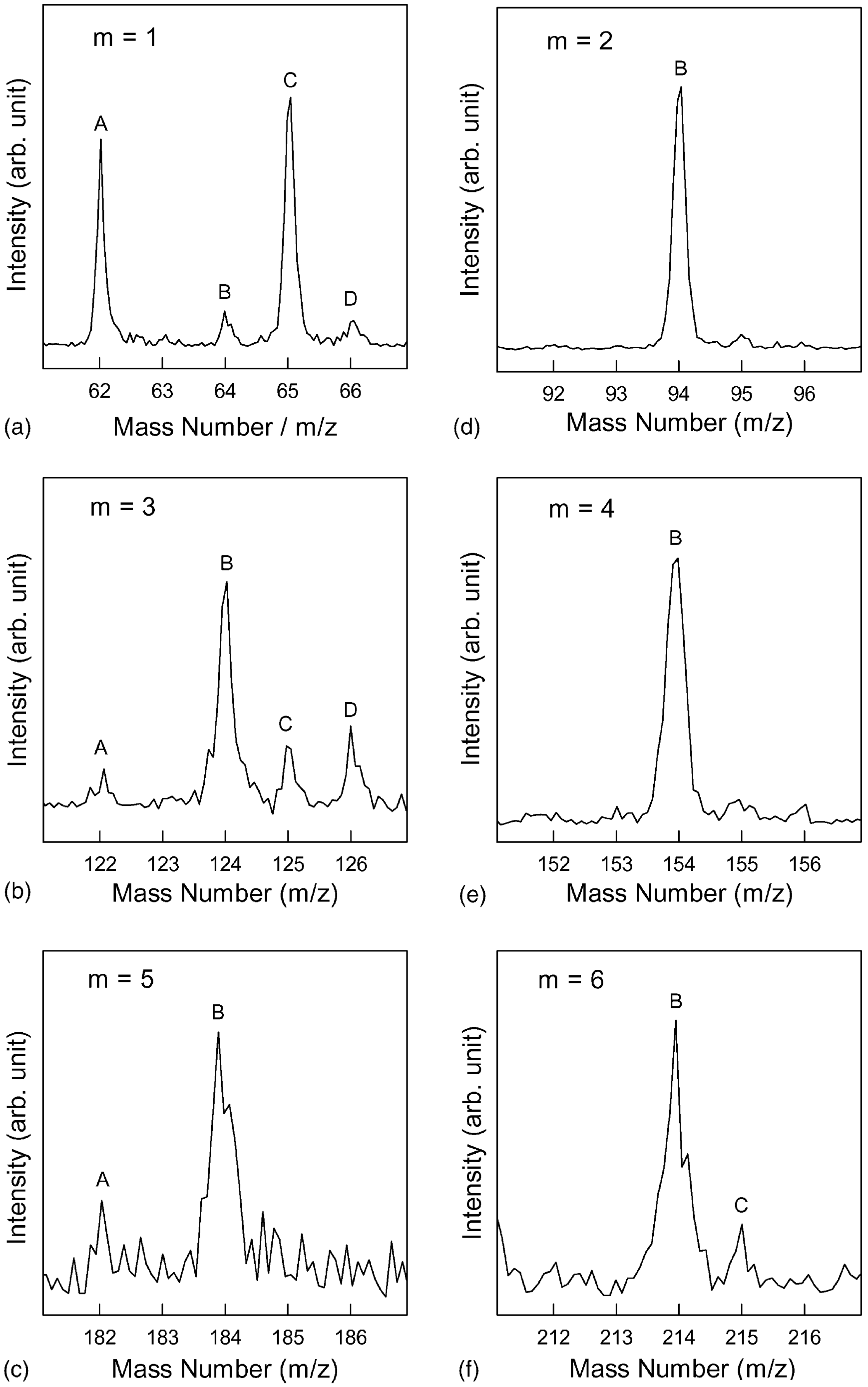

Fig. 4. Mass spectrum obtained from NO (5%) and CD_3OH (0.20%) mixture seeded in 3.1 atm of Ar carrier gas. The different panels indicate cluster ions of the form $[(NO)_m(CD_3OH)]^+$ for $m = 1$–6. The peaks labeled are identified as follows: (A) $[(NO)_m(CD_2O)]^+$; (B) $[(NO)_m(CD_3O)]^+$; (C) $[(NO)_m(CD_3OH)]^+$; (D) $[(NO)_m(CD_3OH)]H^+$ or $[(NO)_m(CD_3OD)]^+$.

mixture is a crucial factor affecting the final distribution of cluster ion products [40–44].

Beginning at $m/z = 91$, we observe cluster ions, $[(NO)(CH_3ONO)_x]^+$, containing up to 12 methyl nitrite molecules, as shown in Fig. 1. The presence of such a cluster ion series is an indication that the internal energy of the cluster ion is sufficient to result in breaking 12 CH_3O–H bonds, where the bond strength of the O–H bond within the methanol molecule is calculated to be about 110 kcal/mol [45]. Based on these experimental observations, we now discuss two possible mechanisms, which could convert the neutral $(NO)_m(CH_3OH)_n$ clusters into the observed cluster ions $[(NO)(CH_3ONO)_x]^+$. One possible mechanism occurs in a stepwise manner, where the first step is the generation of CH_3O radicals, followed by a radical–radical association to form the CH_3ONO species. The second possible mechanism occurs in a concerted manner, in which the CH_3ONO species appear in a one-step reaction.

The first absorption band of gaseous methanol is in the range of 165–200 nm, centered at 185 nm, and is considered an $n \rightarrow \sigma^*$ transition [46–48]. Studies indicate that an ultraviolet photon will excite the lone pair electron on the oxygen atom into an antibonding orbital oriented in the plane defined by the carbon, oxygen and hydrogen atoms. The corresponding potential energy surface is purely repulsive along the O–H bond [46]. This is consistent with the fact that the major channel of dissociation of the electronically excited methanol molecules produces $CH_3O + H$, plus a small amount of $CH_2OH + H$, even though the latter channel is energetically more favorable [48–50]. As mentioned previously, our study has shown that the selective bond breaking of O–H, rather than C–H, occurs within the cluster environment, which is similar to the product formation of the photodissociation of the methanol molecule [48–50]. Our excitation wavelength of 248 nm is too low in energy to excite the first absorption band of methanol. In this case, a two-photon excitation will lead to absorption into the dissociative excited state of methanol.

The stepwise mechanism may be operative in CH_3ONO formation if the CH_3O species is formed by direct photodissociation, followed by the radical combination reaction with NO to produce the CH_3ONO species. However, the stepwise mechanism suffers from several serious flaws. First, the dissociation process for the generation of the 12 CH_3O radicals within the cluster would require 24, 248 nm photons with a total energy of 1300 kcal/mol. Under the present experimental conditions of a nanosecond laser pulse width and unfocused low laser fluence, it would be highly unlikely that cluster ions containing several methoxy radicals could be formed. Secondly, there are no cluster ions containing CD_3O species, i.e., $[(CD_3O)_x(CD_3OH)_n]^+$, in mass spectra where pure CD_3OH in Ar gas was employed, but protonated methanol clusters $[(CD_3OH)_n]H^+$ are predominantly formed [37]. If any CH_3O radicals are generated within NO/methanol clusters via the direct photodissociation of the CH_3OH moiety, the CH_3O species has access to the following reaction channels:

$$CH_3O + NO \rightarrow CH_3ONO, \quad \Delta E_{rxn} = -41.3\,\mathrm{kcal/mol} \tag{1}$$

$$CH_3O + NO \rightarrow CH_2O + HNO, \quad \Delta E_{rxn} = -29.6\,\mathrm{kcal/mol} \tag{2}$$

$$CH_3O + CH_3O \rightarrow CH_3OH + CH_2O, \quad \Delta E_{rxn} = -83.9\,\mathrm{kcal/mol} \tag{3}$$

$$CH_3O + CH_3O \rightarrow CH_3OOCH_3, \quad \Delta E_{rxn} = -38.2\,\mathrm{kcal/mol} \tag{4}$$

$$CH_3O + CH_3OH \rightarrow CH_3OH + CH_2OH, \quad \Delta E_{rxn} = -6.2\,\mathrm{kcal/mol} \tag{5}$$

$$CH_3O \rightarrow CH_2OH, \quad \Delta E_{rxn} = -6.2\,\mathrm{kcal/mol} \tag{6}$$

With the observation that the formation of methyl nitrite species occurs only within cluster ions, reaction (1) seems to be a likely candidate for the production of methyl nitrite species. At the same time the reactions of CH_3O with NO and with CH_3O can also result in the formation of CH_2O, via disproportionation channels (2) and (3). The existence of the disproportionation channel has been well established by investigations through both the bulk gas phase [51,52] and cluster [53] systems. In our study, the only cluster ions containing CD_2O is $[(NO)(CD_2O)]^+$ as noted in Fig. 3. Higher cluster ions containing one or more CD_2O species are not formed, as indicated in Fig. 4. We have also given careful consideration to possible reactions of CH_3O with CH_3OH, due to the probable presence of a number of CH_3OH molecules around any CH_3O species that would be formed. The reaction of CD_3O with CD_3OH may lead to CD_2OH species in the NO/CD_3OH system. However, evidence for the formation of CD_2OH species is not seen in mass spectra as shown in Figs. 3 and 4.

Although the rearrangement of CH_3O into CH_2OH is also exothermic, ab initio calculation predicts a barrier of 36.0 kcal/mol [54]. As mentioned previously, however, the radical–radical association reaction (1) has no activation energy barrier and is exothermic. This means that the rearrangement of CH_3O to CH_2OH species may be unfavorable compared to radical–radical recombination of CH_3O with NO leading to CH_3ONO.

Thirdly, we noted the phenomenon in our previous study [35] that cluster ions containing the CD_3O species appear to be dependent on the number of NO molecules as well as the electron configuration in the cluster ions. This implies that the number of NO species affects the nature of the generation of CD_3O radicals.

As an alternative to the stepwise mechanism, we propose a concerted mechanism for the generation of the $[(NO)(CH_3ONO)_x]^+$ cluster ions. That is, the reaction is a direct consequence of the cluster environment, in which several molecules may react to generate the CH_3ONO species. This reaction is thought to involve the interaction of the electronegative oxygen atoms of CH_3OH molecules with the initially generated, positively charged nitrogen atoms of the nitric oxide cluster ions. The four-centered structure is similar to the structure of the protonated methyl nitrite [55], but with an additional NO molecule. Therefore, the origin of methyl nitrite species produced within the cluster would be attributed to the clustering of methanol molecules on the surface of ion core consisted of mainly NO molecules [56]. Fig. 5 indicates this possible dissociation pathway between a methanol

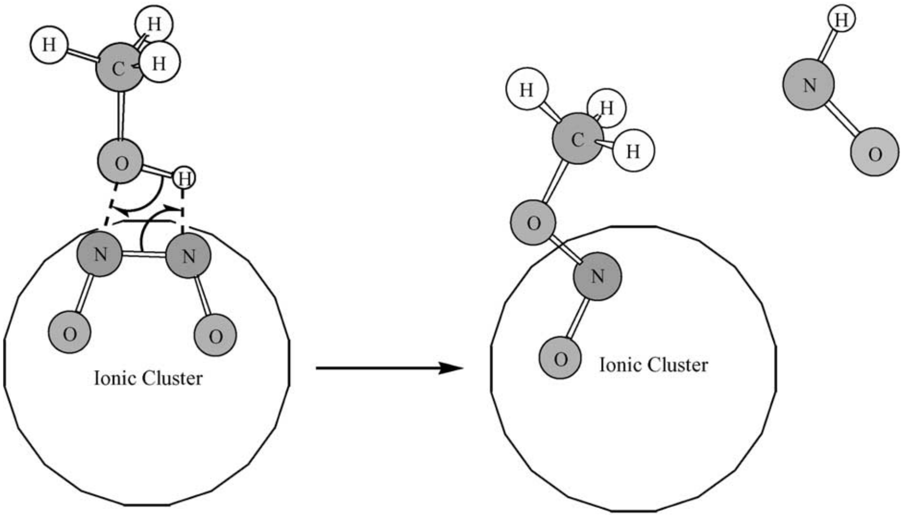

Fig. 5. Schematic drawing indicating the formation of methyl nitrite through the reaction of a methanol molecule with a dimeric unit of NO, within the ionized cluster ions. We assume that the ionic charge resides on the NO species, due to the low ionization potential of NO (IP = 9.265) [57,58] as compared to methanol (10.84 eV) [59]. We also assume that the NO molecules, within the ion cluster, are in the form of dimers, due to the large dimerization energy (0.1 ± 0.02 eV) [57,58].

Table 1
Energy changes in the possible reaction channels of $(NO)_n{}^+$ for $n = 1$, 2 and 3 with CH_3OH molecule[a]

Reactions	ΔE_{rel} (kcal/mol)
$NO^+ + CH_3OH \rightarrow CH_3ONO^+ + H$	133.0
$(NO)_2{}^{+b} + CH_3OH \rightarrow CH_3ONO^+ + HNO$	53.0
$(NO)_3{}^{+b} + CH_3OH \rightarrow NO^+CH_3ONO^c + HNO$	6.0

[a] The heats of formation of some neutral and ionic species are taken from NIST Chemistry WebBook (http://webbook.nist.gov).

[b] Estimated on the basis of the reaction: $NO^+ + NO \rightarrow (NO)_2{}^+$ and $(NO)_2{}^+ + NO \rightarrow (NO)_3{}^+$. For these reactions, the energy changes are found to be −13.79 and −7.36 kcal/mol (see [57,58]), respectively. Combining these values with experimental heats of formation of NO^+ and NO, the heats of formation of $(NO)_2{}^+$ and $(NO)_3{}^+$ are evaluated to be 243.81 and 258.05 kcal/mol, respectively.

[c] Heat of formation can be estimated by a linear relation correlating the bond energy (BE) with the proton affinities (PA). The relation parameters for $NO^+ \cdots X$ were found to be $BE = -36.38 + 0.338PA$ (see [60]), where the energies are expressed in kcal/mol. For $X = CH_3ONO$, BE is calculated as 28.7 kcal/mol which give us the heat of formation for NO^+ CH_3ONO corresponding to 191.7 kcal/mol.

molecule and an NO dimer, within the ionized cluster.

In the NO/CH_3OH cluster system, two photon ionization is energetically possible, since the ionization potential of the mixture should be much smaller that the two-photon energy of the 248 nm wavelength [57,58]. It is expected that the excess energy $[2h\nu - \mathrm{IP(cluster)}] \lesssim 44$ kcal/mol[1] for the initially generated $[(NO)_m(CH_3ONO)_n]^+$ cluster ions would be sufficient to initiate the ion–molecule reaction to generate the methyl nitrite species. As shown in Table 1, the enthalpy changes in the reaction channels decrease with increasing number of NO's. For the reaction of $(NO)_3{}^+$ with a CH_3OH molecule to form $NO^+ \cdots CH_3ONO$ and HNO, we note that the energy change is found to be only slightly endothermic by 6.0 kcal/mol. We note that this energy change is not representative of the energy to form methyl nitrite in the cluster, because it does not include the solvation energy of the reactants. A more appropriate and complete calculation would be to create either the totally dissociated products, or to include the methanol into the reactant ion. This, however, is not a trivial task and is outside of the scope of the current work.

The activation energy of the reaction in these cluster ions is unknown. Either the excess energy given to the cluster ions during the ionization or the additional absorption of photons after ionization, however, should suffice to overcome any activation energy barrier. If enough internal energy remains, additional reactions can take place to generate several methyl nitrite species. Fragmentation of $[(NO)(CH_3OH)_n]^+$ cluster ions [61], suggests their structures are already in the form of $(CH_3OH)_{n-1}H^+ \cdots CH_3ONO$ prior to detection. The separate loss of either NO or CH_3O was not observed. Our own experimental observations have also strongly suggested that the cluster environment enhances production of the methyl nitrite species by: (i) lowering the reaction energy barrier, and (ii) stabilization of the ion–molecule reaction product through either ion–dipole interactions between the ion core and the methyl nitrite species or simple evaporation to lower the internal energy of the cluster ions.

4.2. *Selective chemical reactivity of the O–H bond*

The preference for O–H bond dissociation in the NO/methanol system is in marked contrast to that observed for NO/ethanol clusters [62]. Unlike the NO/methanol system, in NO/ethanol H atom loss occurs from C_α–H fission as well as O–H fission. The most striking feature in the NO/ethanol system is the existence of the critical value of ethanol concentration governing the degree of the participation of the two hydrogen loss channels. Above the critical value of the ethanol concentration, the loss of hydrogen atom from the hydroxyl group is predominant. However, the products generated by the loss of the H atom of the α-carbon begin to appear at the critical value and then rapidly gain in prominence as the ethanol concentration is further decreased.

We have made calculations to elucidate thermochemical data on CH_3ONO, $HOCH_2NO$ and their

---

[1] The bulk ionization energy for nitric oxide is estimated to be about 8.1 eV [57,58]. Therefore, the internal energy of the cluster ions upon two-photon ionization (10 eV) be below 1.9 eV.

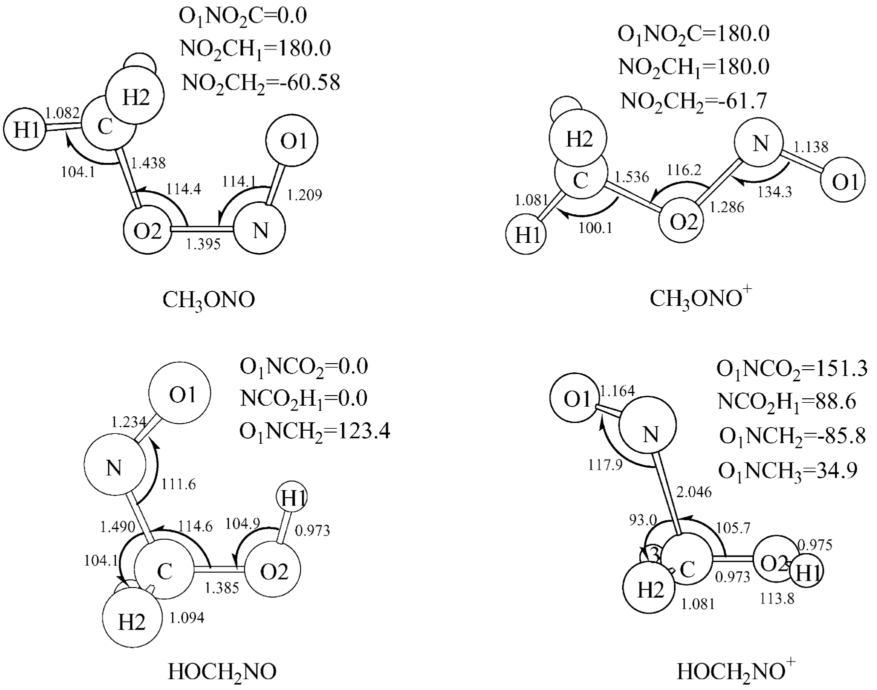

Fig. 6. The global minimum structures for CH_3ONO, $HOCH_2NO$ and their ionic forms optimized at the MP2(full)/6-31G(d,p) level, where bond lengths are given in angstroms (Å) and bond angles in degrees (°).

ionic forms, in an attempt to explain the chemical reactivity of NO/methanol. Hydrogen atom loss from CH_3OH within $[(NO)_m(CH_3OH)_n]^+$ cluster ions may occur either from the hydroxyl position producing CH_3ONO or from the methyl group forming $HOCH_2NO$. The structural and energetic data on these neutral and ionic species have been studied as shown in Fig. 6 and Table 2, where only the global minimum energy structures are addressed in each case. Table 2 indicates that $HOCH_2NO$ is more stable than CH_3ONO at both levels of theory by −3.2 kcal/mol for MP2 and −6.4 kcal/mol for G2. This difference stems mainly from the consequence of the strong hydrogen bonding between the H atom of O–H and the O atom of NO in the $HOCH_2NO$ species, as shown in Fig. 6. Interestingly, the energy difference between the two ionic forms is larger than that of the neutral forms. Like the neural forms, the $HOCH_2NO^+$ ion is calculated to be more stable than CH_3ONO^+, but with a large energy difference of −43.2 and −40.5 kcal/mol at MP2 and G2 levels of theory, respectively. The structure of the $HOCH_2NO^+$ ion exhibits a very long

Table 2
Calculated total energies (hartree) and relative energies Δ*E* (kcal/mol) for CH_3ONO, $HOCH_2NO$ and their ionic forms[a]

Species	MP2(full)/6-31G(d,p)[b]	G2 (298.15 K)	Δ*E* (MP2)	Δ*E* (G2)
CH_3ONO	−244.353526 (0.046340)	−244.674198	0.0	0.0
$HOCH_2NO$	−244.368442 (0.046148)	−244.684445	−3.2	−6.4
CH_3ONO^+	−243.991934 (0.048924)	−244.287972	0.0	0.0
$HOCH_2NO^+$	−244.058697 (0.046847)	−244.352559	−43.2	−40.5

[a] See Fig. 5 for structures.

[b] MP2(full)/6-31G(d,p)//MP2(full)/6-31G(d,p) (with the zero-point vibrational energy contribution in parentheses).

C–N bond, where the charge is mainly centered on CH_2OH (0.82*e*) to the extent that the $HOCH_2NO^+$ ion can be considered as an ion–neutral complex between the CH_2OH^+ ion and the NO molecule. In the case of the CH_3ONO^+ ion, the charge is distributed between the CH_3 (0.64*e*) group and the N (0.75*e*) atom, while the spin densities are localized on NO (0.87*e*). The significant stability in the $HOCH_2NO^+$ ion, compared to the CH_3ONO^+ ion, may be due to the CD_2OH itself having a relatively low ionization potential (7.55 eV) [45], in comparison with those of CH_3O (10.78 eV) [45], CH_3ONO (10.38 eV) [63] and NO (9.265 eV) [57,58].

4.3. Formation of CH_2O species

Another intriguing feature in the NO/CD_3OH system is the appearance of the $[(NO)(CD_2O)]^+$ cluster ion, labeled A in Figs. 3 and 4. It implies that the CD_3OH molecule can undergo loss of both H and D atoms. In a concentration dependence study, the intensity of this peak always surpasses that of the $[(NO)(CD_3O)]^+$ ion and appears to be dependent on the number of NO molecules within the cluster. That is, the formation of the $[(NO)_m(CD_2O)]^+$ clusters appears to depend on the even or odd electron configuration of the resulting cluster ions, much like the even–odd alternation of the ion intensity observed in $(NO)_m{}^+$ cluster ions [58,63–65]. The formation of $[(NO)_m(CD_2O)]^+$ clusters when m = odd is favored by the even-electron configuration.

We note, in the present study, the enhancement in the intensity of the $[(NO)(CD_2O)]^+$ ion compared to either the $[(NO)_3(CD_2O)]^+$ or $[(NO)_5(CD_2O)]^+$ clusters. This observation is in line with the recent work on the collision-induced decomposition (CID) of $[(NO)_p(RO)]^+$ clusters, where these cluster ions preferentially lose NO monomers until they reach the

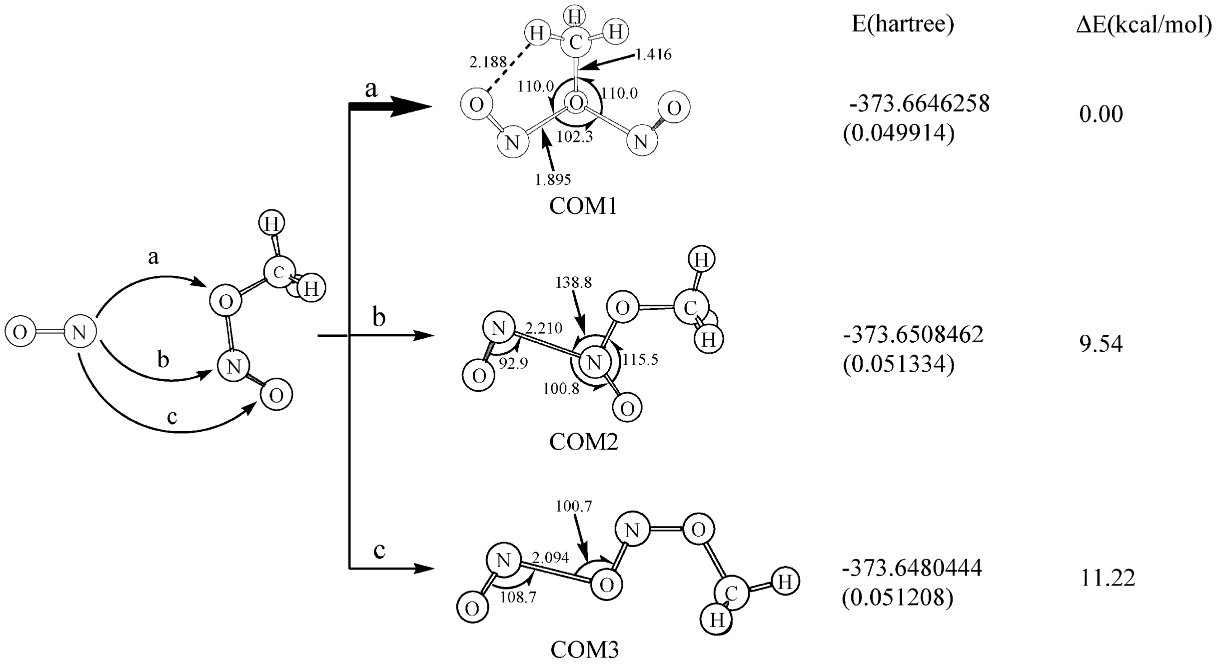

Fig. 7. Schematic drawing illustrating the formation of three potential complexes (COM1, COM2 and COM3) through three routes (a, b and c) in the course of the reaction of NO^+ with CH_3ONO species. Note that each complex also has many relevant conformational isomers. Geometrical parameters for the three complexes are calculated by MP2(full)/6-31G(d,p). Bond lengths are given in angstroms (Å) and bond angles in degrees (°).

$[(NO)_2(RO)]^+$ ion. The next step then is not simply to lose another NO monomer, but rather to undergo an intracluster reaction, expelling HNO producing an aldehyde (R′CHO) within the cluster ion when alcohols such as n-C_2H_5OH, n-C_3H_7OH and n-C_4H_9OH are employed. We therefore propose $[(NO)_p(CD_3O)]^+$ cluster ions, may undergo HNO elimination to generate the observed $[(NO)_m(CD_2O)]^+$ cluster ions, in the following fashion:

$$[(NO)_p(CD_3O)]^+ \rightarrow [(NO)_m(CD_3O)]^+ + (p-m)NO \quad (7)$$

$$[(NO)_p(CD_3O)]^+ \rightarrow [(NO)_m(CD_2O)]^+ + DNO + (p-m-1)NO \quad (8)$$

$$[(NO)_p(CD_3O)]^+ \rightarrow [(NO)_m]^+ + CD_3ONO + (p-m-1)NO \quad (9)$$

Both the present and previous studies [35,66] lead us to believe that reaction channel (7), dominates when $p > 2$, while channels (8) and (9) become predominant only at $p = 2$.

To gain further insight into this process, we have investigated the structure and energetics of the $[(NO)_2(CD_3O)]^+$ cluster. As illustrated in Fig. 7, three different complexes have been calculated, and three different routes are considered in the course of the complex formation between the NO^+ and the CH_3ONO species. Note that only the global minimum energy structure in each complex is reported, even though each complex has many conformers. As shown

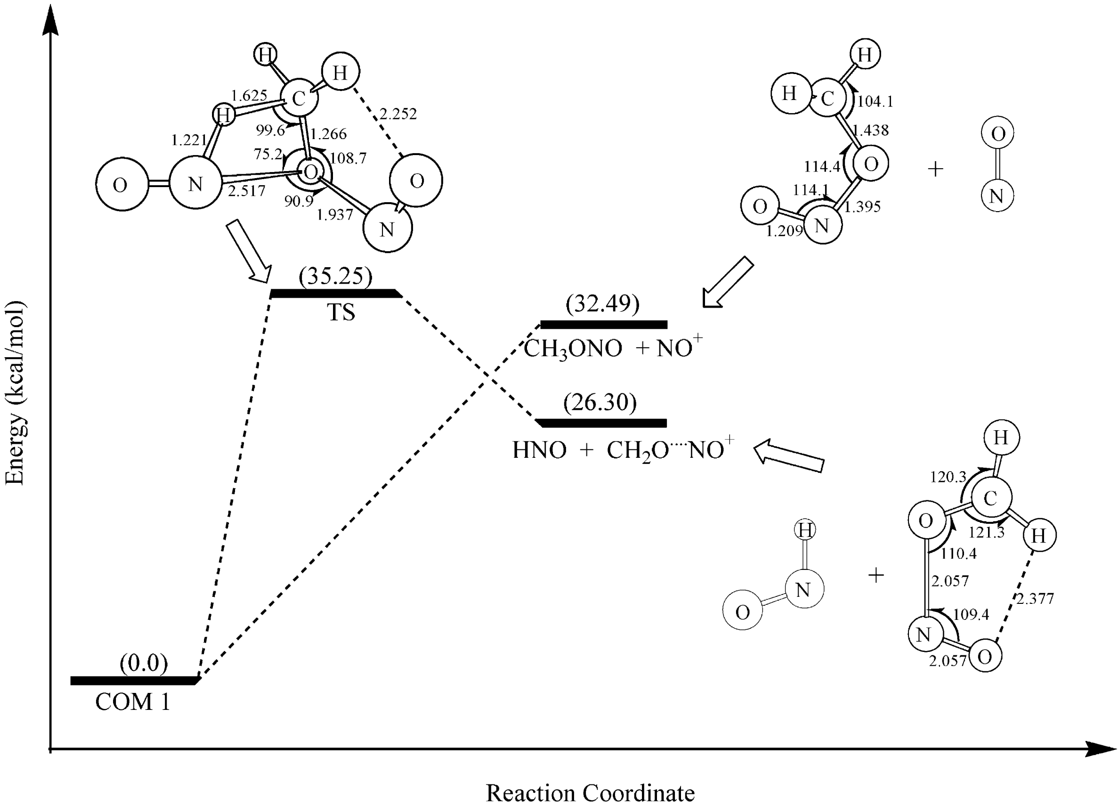

Fig. 8. Potential energy surface diagram for the decomposition of the most stable complex ionic form, COM1, into $CH_3ONO + NO^+$ and $HNO + CH_2O \cdots NO^+$. Energy levels are given relative to that of COM1 including zero-point vibrational energy (ZPVE) correction at the MP2(full)/6-31G(d,p) level of theory.

in Fig. 7, the most stable one is labeled COM1, which can be characterized as a complex consisting of three distinct components, i.e., $[ON \cdots O(CH_3) \cdots NO]^+$. Such a geometry lowers the energy by 9.6 and 11.2 kcal/mol in contrast to the other two complexes, COM2 and COM3, which are $[ON \cdots N(O)OCH_3]^+$ and $[ON \cdots ONOCH_3]^+$, respectively. We note that COM1 is capable of both HNO elimination as well as the CH_3ONO dissociation channels. This then prompted us to select COM1 as the reaction structure to explore the dissociation of the $[(NO)_2(CH_3O)]^+$ cluster.

The potential energy surface of COM1 is depicted in Fig. 8. Only two reaction channels, forming CH_3ONO plus NO^+ and HNO plus $CH_2O \cdots NO^+$, have been considered in this study[2]. The lowest energy path is the formation of HNO plus $CH_2O \cdots NO^+$. As shown in Fig. 8, the transition state, connecting COM1 and HNO plus $CH_2O \cdots NO^+$, is only ∼2.8 kcal/mol above the channel yielding CH_3ONO plus NO^+. The channel forming HNO plus $CH_2O \cdots NO^+$ is less endothermic than the channel yielding CH_3ONO plus NO^+ by ∼6.2 kcal/mol. It is reasonable to predict that such a close energy difference can lead to competition between these two channels.

4.4. Implications for the non-thermal plasma chemistry

As mentioned in the introduction, there have been extensive investigations on abating the emission of trace air pollutants into the atmosphere by using non-thermal plasma processes. The basic principle of these techniques is to generate chemically reactive species such as excited molecules, atoms, radicals and ions through electron impact ionization and dissociation. A majority of the energy goes into the production of energetic electrons, rather than into background gas heating. In these processes, the generated ions take part in the chemical processes responsible for the removal of the air pollutants. Our results indicate that there is the undesirable possibility of generating the CH_3ONO species as an unwanted by-product, if methanol is used as an additive in the non-thermal plasma techniques.

5. Conclusion

We have studied the heterogeneous NO/CH_3OH cluster system and observed: (1) the formation of ionic clusters containing as many as 12 methyl nitrite molecules; and (2) the complete conversion of neutral $(NO)_n(CH_3OH)_m$ clusters into methyl nitrite cluster ions of the form $[(NO)(CH_3ONO)_x]^+$ mediated by the cluster environment. Based upon the experimental and calculational results, it is proposed that the formation of the methyl nitrite species within the cluster proceeds through a concerted mechanism. Methyl nitrite cluster ions are formed exclusively in spite of calculations that indicate that the $HOCH_2NO^+$ ion is lower in energy than the CH_3ONO^+ ion.

Acknowledgements

We acknowledge the past support of the National Science Foundation through grant number NSF/ATM-9711381. D.N.S. is grateful to the Korea Science and Engineering Foundation (KOSEF) for partial financial support.

References

[1] B.J. Finlayson-Pitts, J.N. Pitts Jr., Science 276 (1997) 1045.
[2] R.K. Lyon, Environ. Sci. Technol. 21 (1987) 231.
[3] R.A. Perry, D.L. Siebers, Nature 324 (1986) 657.
[4] M. Shelef, Chem. Rev. 95 (1995) 209.
[5] P. Gilot, M. Guyon, B.R. Stanmore, Fuel 76 (1997) 507.
[6] J. Newhall Pont, A.B. Evans, G.C. England, R.K. Lyon, W.R. Seeker, Environ. Prog. 12 (1993) 140.
[7] P.R. Courtry, A. Chauvel, Catal. Today 29 (1996) 3.
[8] K. Kawamura, S. Aoki, H. Kimura, K. Adachi, K. Kawamura, T. Katayama, K. Kengaku, Y. Sawada, Environ. Sci. Technol. 14 (1980) 288.
[9] H. Matzing, Adv. Chem. Phys. 80 (1991) 315.
[10] B.M. Penetrante, S.E. Schultheis, Non-thermal Plasma Techniques for Pollution Control: Part A—Overview, Fundamentals and Supporting Technologies, Springer-Verlag, Heidelberg, 1993.

---

[2] In our previous study [66], it was found that three channels takes part in the dissociation of $[(NO)_2(CH_3CH_2O)]^+$ ions. However, the channel yielding CH_3CH_2O plus $(NO)_2{}^+$ is trivial in comparison with the other channels.

[11] B.M. Penetrante, S.E. Schultheis, Non-thermal Plasma Techniques for Pollution Control: Part B—Electron Beam and Electrical Discharge Processing, Springer-Verlag, Heidelberg, 1993.

[12] B.M. Penetrante, J.N. Bardsley, M.C. Hsiao, Jpn. J. Appl. Phys. 36 (1997) 5007.

[13] J.A. Miller, C.T. Bowman, Prog. Energy Combust. Sci. 15 (1989) 287.

[14] J.A. Miller, G.A. Fisk, Chem. Eng. News 8 (1987) 22.

[15] K. Yan, S. Kanazawa, T. Ohkubo, Y. Nomoto, Plasma Chem. Plasma Process. 19 (1999) 421.

[16] Y.H. Song, W.H. Shin, Y.S. Choi, S.J. Kim, J. Adv. Oxid. Tech. 2 (1997) 268.

[17] B.K. Gullet, P.W. Groff, M.L. Lin, J.M. Chen, J. Air Waste Manage. Assoc. 44 (1994) 1188.

[18] L.A. Rosocha, S.J. Kim, K. Urashima, J.-S. Chang, A.W. Miziolek, M.J. Nusca, R.G. Daniel, J.T. Herron, in: Proceedings of the Asia-Pacific Workshop on Water and Air Treatment by Advanced Oxidation Technologies: Innovation and Commercial Application, Tsukuba, Japan, 1998, p. 195.

[19] T. Oda, T. Kato, T. Takahashi, K. Shimizu, IEEE Trans. Ind. Appl. 34 (1998) 268.

[20] J. Luo, S.L. Suib, M. Marquez, Y. Hayashi, H.J. Matsumoto, Phys. Chem. A 102 (1998) 7954.

[21] Y.S. Mok, I.S. Nam, J. Chem. Eng. Jpn. 31 (1998) 391.

[22] J.Y. Park, I. Tomicic, G.F. Round, J.S. Chang, J. Phys. D: Appl. Phys. 32 (1999) 1006.

[23] E.M. Van Veldhuizen, L.M. Zhou, W.R. Rutgers, Plasma Chem. Plasma Process. 18 (1998) 91.

[24] A. Mizuno, M. Kurahashi, S. Imano, T. Ishida, M. Nagata, in: Proceedings of the IEEE Ind. Appl. Soc. Annual Meeting, New Orleans, 1997, p. 2032.

[25] L. Civitano, in: B.M. Penetrante, S.E. Schultheis (Eds.), Non-thermal Plasma Techniques for Pollution Control: Part B—Electron Beam and Electrical Discharge Processing, Springer-Verlag, Heidelberg, 1993, p. 103.

[26] S.G. Masters, D. Chadwick, Catal. Today 42 (1998) 137.

[27] V.M. Zmansky, L. Ho, P.M. Maly, W.R. Seeker, Combust. Sci. Technol. 120 (1996) 255.

[28] R.K. Lyon, J.A. Cole, J.C. Kramlich, S.L. Chen, Combust. Flame 81 (1990) 30.

[29] H.-R. Paur, S.J. Jordan, Aerosol Sci. 20 (1989) 7.

[30] B.V. Potapkin, M.A. Deminsky, A.A. Fridman, V.D. Rusanov, in: B.M. Penetrante, S.E. Schultheis (Eds.), Non-thermal Plasma Techniques for Pollution Control: Part A—Overview, Fundamentals and Supporting Technologies, Springer-Verlag, Heidelberg, 1993, p. 91.

[31] H. Matzing, H.-R. Paur, H.J. Bunz, Aerosol Sci. 19 (1988) 883.

[32] F.C. Fehsenfeld, M. Mosesman, E.E. Ferguson, J. Chem. Phys. 55 (1971) 2120.

[33] F.C. Fehsenfeld, C.T. Howard, A.L. Schmeltekopf, J. Chem. Phys. 63 (1975) 2835.

[34] A.J. Stace, J.F. Winkel, R.B. Lopez Martens, J.E. Upham, J. Phys. Chem. 98 (1994) 2012.

[35] D.N. Shin, R.L. DeLeon, J.F. Garvey, J. Chem. Phys. 110 (1999) 5564.

[36] M.Y. Lykety, P. Xia, J.F. Garvey, Chem. Phys. Lett. 238 (1995) 54.

[37] P. Xia, M. Hall, T.R. Furlani, J.F. Garvey, J. Phys. Chem. 100 (1996) 12235.

[38] Gaussian 98, Revision A.9, Gaussian, Inc., Pittsburgh, PA, USA, 1998.

[39] L.A. Curtiss, K. Raghavachari, G.W. Trucks, J.A. Pople, J. Chem. Phys. 94 (1991) 7221.

[40] Y. Akiyama, A. Wakisaka, F. Mizukami, K.J. Sakaguchi, Chem. Soc., Perkin Trans. 2 (1998) 95.

[41] M.Z. Martin, S.R. Desai, C.S. Feigerle, J.C. Miller, J. Phys. Chem. 100 (1996) 8170.

[42] W.B. Tzeng, S. Wei, D.W. Neyer, R.G. Keesee, A.W. Castleman Jr., J. Am. Chem. Soc. 112 (1990) 4097.

[43] D.N. Shin, K.W. Jung, K.-H. Jung, J. Am. Chem. Soc. 114 (1992) 6926.

[44] D.N. Shin, C.J. Choi, K.-H. Jung, K.W. Jung, Bull. Kor. Chem. Soc. 17 (1996) 939.

[45] S.-C. Kuo, Z. Zhang, R.B. Klemm, J.F. Liebman, L.J. Stief, F.L. Nesbitt, J. Phys. Chem. 98 (1994) 4026.

[46] D.R. Salahub, C. Sandorfy, Chem. Phys. Lett. 8 (1971) 71.

[47] M.B. Robin, Higher Excited States of Polyatomic Molecules, Vol. 1, Academic Press, New York, 1974.

[48] C. von Sonntag, in: S.P. McGlynn (Ed.), Photophysics and Photochemistry in the Vacuum Ultraviolet, Reidel, New York, 1985, p. 913.

[49] S. Satyapal, J. Park, R. Bersohn, B. Katz, J. Chem. Phys. 91 (1989) 6873.

[50] Y. Wen, J. Segall, M. Dulligan, C. Wittig, J. Chem. Phys. 101 (1994) 5665.

[51] F. Caralp, M.-T. Rayez, W. Forst, N. Gomez, B. Delcroix, C. Fittschen, P. Devolder, J. Chem. Soc., Faraday Trans. 94 (1998) 3321.

[52] S. Dobe, G. Lendvay, I. Szilagyi, T. Berces, Int. J. Chem. Kinet. 26 (1994) 887.

[53] K. Bergmann, J.R. Huber, J. Phys. Chem. A 101 (1997) 259.

[54] S. Saebo, L. Radom, H.F. Schaefer III, J. Chem. Phys. 78 (1983) 845.

[55] M. Aschi, F. Grandinetti, Chem. Phys. Lett. 258 (1996) 123.

[56] A. Stace, J. Org. Mass Spectrom. 28 (1993) 3.

[57] S.H. Linn, Y. Ono, C.Y. Ng, J. Chem. Phys. 74 (1981) 3342.

[58] S.R. Desai, C.S. Feigerle, J.C. Miller, J. Chem. Phys. 97 (1992) 1793.

[59] J. Momigny, H. Wankenne, C. Krier, Int. J. Mass Spectrom. Ion Phys. 35 (1980) 51.

[60] H. Wincel, Chem. Phys. Lett. 292 (1998) 193.

[61] J.F. Winkel, A.J. Stace, Chem. Phys. Lett. 221 (1994) 431.

[62] D.N. Shin, R.L. DeLeon, J.F. Garvey, J. Am. Chem. Soc. 122 (2000) 11887.

[63] J.P. Gilman, T. Hsieh, G.G. Meisels, J. Chem. Phys. 78 (1983) 3767.

[64] L. Poth, Z. Shi, Q. Zhong, A.W. Castleman Jr., J. Phys. Chem. A 101 (1997) 1099.

[65] A. Mouhandes, A.J. Stace, J. Chem. Phys. 111 (1999) 9517.

[66] J.P. Charlebois, R.L. DeLeon, J.F. Garvey, J. Phys. Chem. A 104 (2000) 6799.